Engineering Journal issn: 0125-8281

Article

Seismic Retrofit of Central Opening Partial Infilled Frame by Expanded Metal Ferrocement

Phaiboon Panyakapo

Civil Engineering and Urban Development Department, Engineering Faculty, Sripatum University, Thailand
E-mail: phaiboon.pa@spu.ac.th

Abstract. This paper presents the retrofit of partial infilled frame with central opening by ferrocement and expanded metal. Theoretical models are suggested to design the lateral resistance of the retrofitted frames. Experimental tests on the prototype frames were carried out to verify the design method. Four specimens were built to the full scale, which were divided into two groups: a) the bare frame and the retrofitted frame, and b) the partial infilled frame with window opening and the retrofitted frame. It was found that the retrofitted frame with window opening showed satisfactory behaviors including the lateral strength, lateral stiffness and energy dissipation capacity. The observed maximum lateral strength of the retrofitted frame with opening achieved the design strength. The proposed model predicted the lateral strength with a good accuracy when it was compared with the experimental result. The strengthened columns for the opening infilled frame prevented brittle shear failure due to the behavior of short column. The retrofitted column exhibited a ductile behavior with the developed flexural crack at the constrained level.

Keywords: Seismic retrofit, partial infilled frame, window opening, expanded metal.

ENGINEERING JOURNAL Volume 29 Issue 2
Received 23 September 2024
Accepted 29 January 2025
Published 28 February 2025
Online at https://engj.org/
DOI:10.4186/ej.2025.29.2.45

DOI:10.4186/ej.2025.29.2.45

1. Introduction

Lessons from the 2014 Earthquake in Chiang Rai located in the northernmost of Thailand revealed that many existing buildings containing brick wall panel in the reinforced concrete frame were severe destroyed due to the interaction effect of frame and infill panel [1]. It was observed for solid infill panel that failure mode was due to diagonal stress of brick wall causing diagonal crack of the brick wall. On the other hand, for the case of infill panel with opening, the presence of openings significantly affected to the surrounding frame. Failure modes of the reinforced concrete frames include [2]: flexural yielding of frame components, lap-splice slip in concrete, concrete shear failure, and concrete joint failure. Among these, concrete shear failure is the major form of damage because the ability of the column to carry axial load may be seriously impaired. The damages due to the presence of the window openings for the infilled frames with partial height of wall panel are shown in Figs. 1(a)- 1(b). The infill panels restricted the ability of columns to deform laterally by partially confining of the lower wall portion. Thus, the large shear force transferred to the columns resulting in shear failure due to the behavior of short-column. This building was demolished and reconstructed due to unrepairable damage of columns, resulting in susceptible to collapse of the whole building. Therefore, seismic retrofit of the existing infilled frames with opening is required.

a) crack of column b) shear failure of column

Fig. 1. Damage of columns due to short column effect for infilled frame with openings .

Several techniques have been proposed to improve the infilled frame with opening [3-6]. The mortar mixed with textile material was employed to retrofit the infilled frame with a central door opening [7]. The method could improve the lateral resistance, stiffness, and deformation capacity. The efficiency of the technique was dependent on the layers and the locations of the retrofitted materials. The CFRP was also investigated for retrofitting the infilled frames with various sizes and locations of openings [8]. The large size of opening reduced the load capacity. While the central location of opening provided greater load capacity than the corner location. It was reported that the strength of masonry walls has an influence on the effectiveness of FRP [9]. The masonry walls with medium strength provided the optimum efficiency because the failure occurred in the zone where the FRP was installed. Although FRP technique is widely used due to its lightweight and high strength material. The use of CFRP for retrofitting the infilled frames could increase the stiffness up to 2.7 times [10]. However, some difficulties may arise during the application of FRP on the infilled frame, these include: debonding of FRP strip when high stress concentration occurs at the FRP anchorage including inconsistency between brick wall and epoxy resin, and the necessity for surface preparation and sensitivity to the effect of fire [11].

As an alternative, the technique of ferrocement with expanded metal bonded with mortar plastering was found to be effective due to their high adhesive strength. Typically, there are two types [12]: standard type, in which the bars like rhomb shape are connected by overlapping, and flattened type, which forms a completely flattened sheet without overlap between stitches. Several researches on the seismic retrofit with expanded metal have been conducted. For example, the expanded steel meshes have been employed to strengthen the reinforced concrete columns with ferrocement jacket [13]. It was found that the shear strength of the retrofitted columns could be increased, resulting in a significant increase of ductility capacity. The investigation on the shear strength of expanded metal sheets revealed that the hysteretic behaviors of the specimens were stable with large hysteresis loops, leading to an improvement of ductility capacity up to 10 [14]. However, the pinching effects caused a stiffness degradation due to the buckling of the compression bars of the metal sheet. In addition, the results of quasi-static load tests showed that shear strength of the mesh depended on the mesh shape and the panel length [15]. The application of expanded metal to retrofit the brick infilled frame was investigated [16]. The brick wall strengthened with expanded metal sheet and cement mortar in the form of ferrocement could enhance the lateral resistance, stiffness and energy dissipation. Further study on the strengthening technique of brick wall and beam-column frame was conducted [17]. It was found that the retrofit method of ferrocement for brick wall by using steel plate at the wall corners could prevent the failure of columns due to the corner compression of the wall. On the other hand, a similar type of expanded metal was employed by using steel plate with perforated panel to strengthen the walls [18]. The strengthened specimens could increase the strength and ductility compared with the reference sample. However, the specimens were limited to the strengthening of solid infill wall without plastering.

Several researches on the strengthening technique of ferrocement reinforced with expanded metal mesh were investigated. The columns confined with ferrocement were tested for shear strength of short columns [19]. The variation of expanded metal sizes revealed that the increase of mesh size could improve the displacement ductility as well as shear strength of the retrofitted columns. Similar experimental study on the confinement

of columns using steel cage technique was conducted [20]. The steel angles were attached at each corner of column and connected with steel batten at several spacings along the column. The test results showed that the external confinement of column increased the strength, stiffness, energy dissipation and ductility of the strengthened columns. However, the weld connection of steel members requires careful workmanship to achieve a good quality of steel connection. A comparison of this ferrocement technique between an interlocking block and the conventional concrete block was conducted with a variation of mesh sizes [21]. The results showed that the interlocking block with ferrocement provided greater strength and ductility than the others. The small mesh sizes were superior to the large mesh due to the increase of specific surface of mesh. For the application of this retrofit method to the structures, seismic performance of school building strengthened with steel batten reinforced with expanded metal was studied [22]. The retrofit technique could improve the strength and initial stiffness of the building. The damage at the plastic hinge region of the beams and columns was diminished.

However, previous studies have not investigated the strengthening of opening infilled frame by expanded metal sheet, especially for partial infill panel with the presence of window opening. In this study, the typical infilled frame with partial height of masonry panel due to the presence of a wide window opening was selected. Four specimens of frames were investigated, these include: the controlled bare frame (F), the retrofitted bare frame (F-R), and the controlled infilled frame with central opening (FO) and the retrofitted frame (FO-R). The theoretical models for retrofitting bare frame and the infilled frame with central opening were proposed to design the lateral resistance of the retrofitted frames. The experimental tests on the strengthened frames under cyclic loading were conducted to verify the proposed design method.

2. Prototype Structure

In this study, the typical school building which is the standard of the Ministry of Education was selected to represent for the infilled frame. The detailed design of the structure was determined according to EIT 1007-34 [23] without seismic detailing, similar to ACI 318-95 [24]. The standard school building is shown in Fig. 2a. The selected infilled frame with window at the central part is presented in Fig. 2b. The infill panel is divided into two parts, i.e., the upper and the lower panels. The upper infill wall was supported by a lintel beam with reinforcing bars connected to each side of the column. The window opening is a wide frame spanning through the clear distance of columns, located at the center of the infill panel. Since the upper and the lower infill panels reduce the clear height of the adjacent columns, the effect of short column which leads to shear failure of columns is inevitable. Therefore, it is required to strengthen the infilled frame with opening. The retrofit scheme is divided into two parts: a) bare frame, and b) infilled frame with opening.

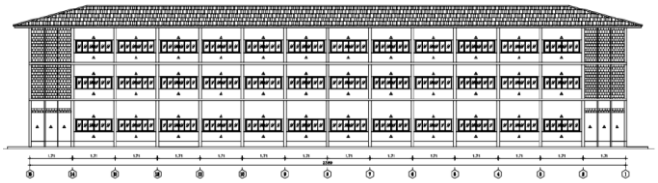

a) Elevation

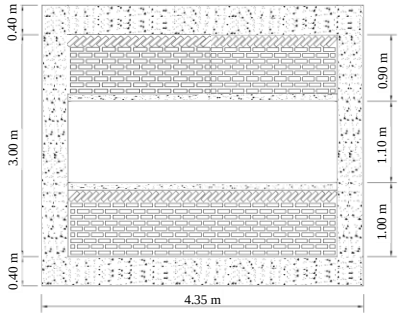

b) Infilled frame with window opening

Fig. 2. Standard school building.

3. Models for the Retrofitted Frames

In this section, the theoretical models are presented to evaluate the lateral resistance of the retrofit frames: a) bare reinforced concrete frame and b) central opening partial brick infilled frame. The suggested method is employed for the design of the retrofit frames in the next section.

3.1. Retrofitted Bare Frame

The reinforced concrete frame and the detailed section of the retrofitted column are shown in Figs. 3a-3b. The ferrocement technique was applied with expanded metal as the reinforcement. The expanded metal sheets were attached at each side of column connecting with steel angels at the corners of column. The connection was performed by welding between the edge of steel angle and the mesh reinforcement.

From Figs. 3c-3d, the strains and forces due to the confinement are presented along the cross-section of the column. To calculate the bending moment strength of the retrofitted column (M_R), the ultimate moment of ferrocement (M_F) is combined with that of the existing column (M_E) as presented in Eq. (1):

$$M_R = M_E + M_F \quad (1)$$

where M_F can be determined by taking the moment from the tensile forces of the expanded metal (T_e) and the steel angle (T_a) to the center of compressive stress block. This calculation is based on the basic assumption that the moments due to the compressive forces of expanded

DOI:10.4186/ej.2025.29.2.45

metal and steel angle are very small and it can be neglected as suggested by ACI549.1R [25].

$$M_F = T_e\left(d_1 - \frac{a}{2}\right) + T_a\left(d_2 - \frac{a}{2}\right) \quad (2)$$

The tensile force of the expanded metal is calculated by using the effective area of reinforcement [25].

$$T_e = \eta V_f A_c f_e \quad (3)$$

where η is the efficiency factor (0.65), V_f is the ratio of volume of reinforcement and ferrocement, A_c is cross section area of cement mortar, and f_e is the tensile strength of reinforcement corresponding to the strain ε_e. The tensile force of the steel angle can be taken as:

$$T_a = \eta A_s F_a \quad (4)$$

where A_s, f_a is cross section area and the tensile strength of steel angle corresponding to the strain ε_a, respectively. The lateral resistance of the bare frame can be obtained by the shear force resulting from the moment capacity of the column over its height. Therefore, the lateral resistance of the retrofitted bare frame (R_{BF}) is the shear force resulting from the sum of moments of the joint connection (M_{pj}), existing column (M_E) and the ferrocement reinforcement M_F:

$$R_{BF} = \frac{2(M_{pj} + M_R)}{L} = \frac{2\left(M_{pj} + M_E + M_F\right)}{L} \quad (5)$$

where M_{pj} is the moment at the joint determined by the minimum moment of beam (M_{pb}), column (M_{pc}), the beam-column connection.

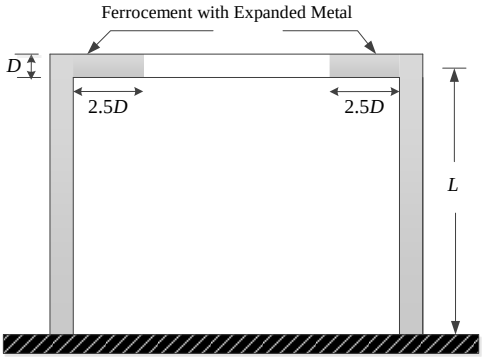

a) Bare Frame

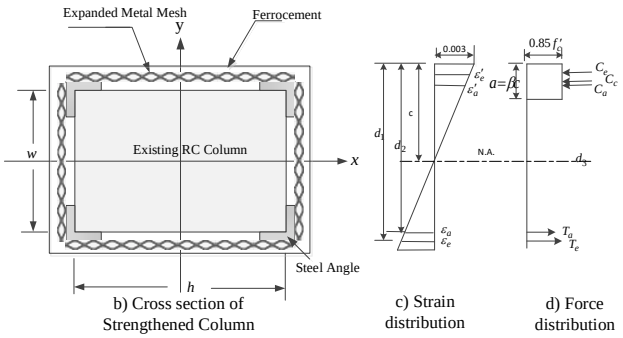

Fig. 3. Retrofitting of bare frame.

3.2. Partial Infilled Frame

The infilled frame containing an opening of window located at the center of the brick wall was selected as the prototype frame, as shown in Fig. 4. The beam-column reinforced concrete frame was strengthened by the ferrocement technique. The infill panel was divided into two parts due to the presence of a window opening, i.e., the upper and the lower panels with the wall height of h_1 and h_2, respectively, and the height of central opening h_o. Both parts of infill panels were strengthened by the ferrocement technique reinforced with expanded metal. For each infill panel, the common form of failure mode is diagonal cracking, one may assume that the force of the equivalent strut of each wall panel is primarily dominated by the diagonal strut in compression.

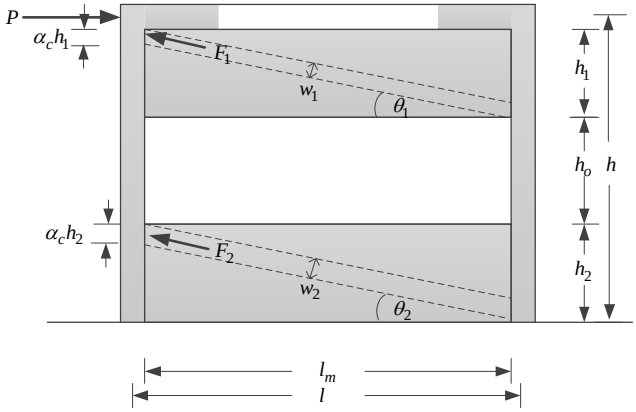

Fig. 4. Diagonal struts for infilled frame with opening.

From the force equilibrium, the lateral applied force P is equal to a combination of the bare frame resistance R_{BF} and the lateral force components of F_1 and F_2, as shown in Eq. (6).

$$P = R_{BF} + F_1\cos\theta_1 + F_2\cos\theta_2 \quad (6)$$

where F_1 and F_2 are represented for the diagonal strut force for the upper and the lower panels, respectively, which can be calculated as follows:

$$F_1 = w_1 t f_a \quad (7)$$

$$F_2 = w_2 t f_a \tag{8}$$

where f_a is the allowable stress of masonry prism, which may be calculated as $f_a = 0.6\phi f_m^{'}$, ϕ=0.65, $f_m^{'}$ is the masonry prism strength, t is the thickness of masonry infill wall, and θ_1, θ_2 are the inclination angles of the diagonal strut for the upper and the lower panels, respectively.

The strut widths of the upper and the lower masonry panels can be determined from the stress distribution at the interface of frame and wall [26]:

$$w_1 = \alpha_c h_1 \frac{l_m}{\sqrt{h_1^2 + l_m^2}} = \alpha_c h_1 \cos\theta_1 \tag{9}$$

$$w_2 = \alpha_c h_2 \frac{l_m}{\sqrt{h_2^2 + l_m^2}} = \alpha_c h_2 \cos\theta_2 \tag{10}$$

$$\alpha_c = \frac{1}{h}\sqrt{\frac{2M_{pj} + 2\beta_c M_{pc}}{\sigma_c t}} \tag{11}$$

$$\sigma_c = \frac{f_m'}{\sqrt{1 + 3\mu^2 r^4}} \tag{12}$$

μ represents friction factor of the beam-column and infill panel, r is the height/length relation of the rigid frame, β_c is referred to the multiplying factor of column (0.2).

4. Tet Setup of the Prototype Frame

4.1. Bare Frame (F)

The selected bare frame at the central of the standard school building was modelled and prepared for experimental test. The prototype frame is shown in Fig. 5. The dimensions of beams, columns, and reinforcing bars were selected from the frame located at the ground floor elevation of the central part of the standard school building, the Ministry of Education. The mechanical properties of concrete and reinforcing steel of the bare frame are normal strength, i.e., concrete with 24 Mpa cylindrical compressive strength (f_c') and the rebar with 240 Mpa yield strength (f_y). The dimensions of column and beam are 0.35×0.45 m and 0.20×0.40 m, respectively, which indicates that the bare frame is weak beam-strong column. The reinforcement details are vulnerable for seismic resistance, i.e., wide spacing of the tie reinforcement of the column as well as the stirrup of the beam with 90 degree hook, and the lap splices of the longitudinal bars of the columns are located at the lower end. This indicates that low shear strength of the beam and column components under cyclic loading might be expected. The bare frame specimen was prepared for full scale load test.

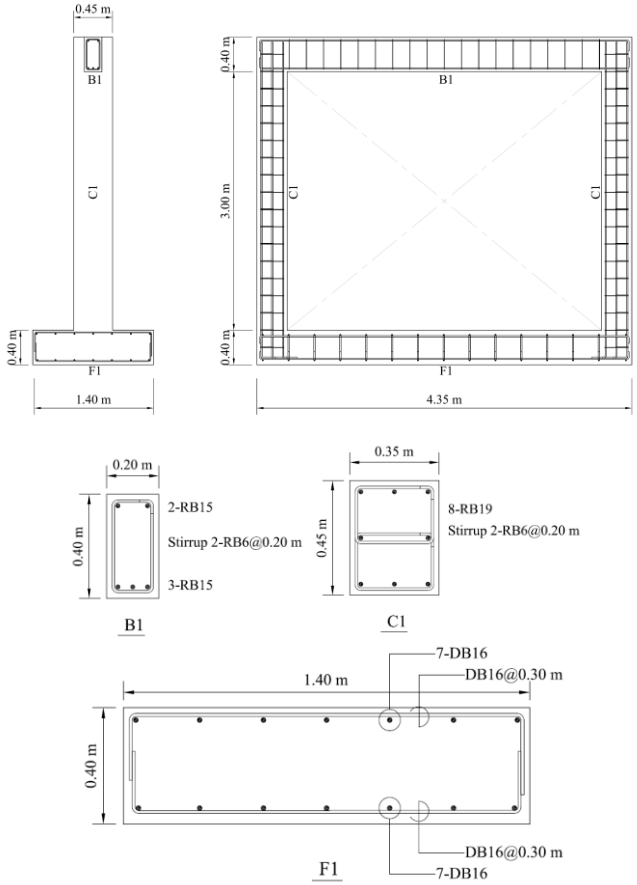

Fig. 5. Prototype reinforced concrete bare frame.

4.2. Retrofitting of Bare Frame (F-R)

The retrofitted bare frame (F-R) was designed based on an assumption that the lateral resistance of the strengthened bare frame is 1.5 times that of the existing bare frame (F). The theoretical model of the strengthened bare frame described in the preceding section was employed in the calculation. The strengthening technique is ferrocement reinforcing with expanded mental. The expanded metal sheet is EMS diamond mesh corresponding to JIS G3351 [27]. For column and beam, the type-1 expanded metal was chosen for the reinforcement. For brick infill panel, the steel mesh type-2 was chosen for laminating infill panel. The characteristics of expanded metal sheet are shown in Figs. 6a, 6b and Table 1, respectively. The tensile strengths f_y and f_u of the steel bar are 340 Mpa and 400 Mpa, respectively [10]. In the retrofitting process, since the diamond mesh in the long way (LW) is stronger than the short way (SW), the LW diamond mesh was placed parallel to the direction of shear force to be resisted. Therefore, the LW mesh was located perpendicular to the axial axis of column and beam. This is intended to improve the shear strength of the column and beam. The expanded metal sheets were welded to the steel angels at each side of the columns. The strengthened bare frame and the detailed connection between the steel angle and the expanded metal sheet are shown in Figs. 6c, 6d, respectively.

DOI:10.4186/ej.2025.29.2.45

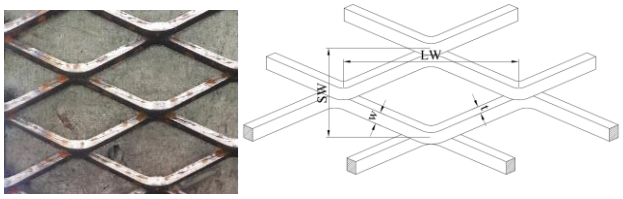

a) Expanded metal sheet b) Enlarged mesh

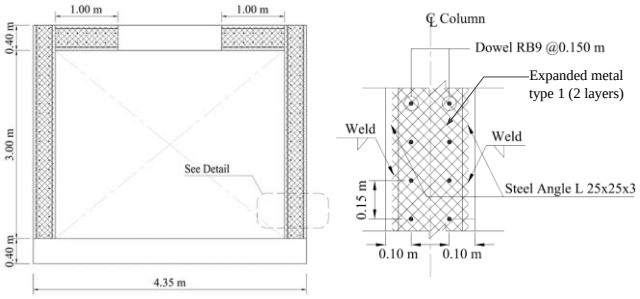

c) Strengthened bare frame d) Detailed connection

Fig. 6. Expanded metal mesh and detailed connection for the bare frame.

Table 1. Characteristics of the selected Expanded Metal.

Mesh Types	SW (mm)	LW (mm)	t (mm)	w (mm)
Type -1	34.0	76.2	4.5	4.5
Type-2	8.6	20.0	0.6	0.6

4.3. Infilled Frame with Central Opening (FO)

The central opening infilled frame, which represents for the controlled specimen, is composed of reinforced concrete frame and two parts of infill panel. The same type of bare frame was employed for the RC frame. The infill panel was constructed with half brick 65 mm. thickness. The compressive strength of brick was 3.5 Mpa according to ASTM C170-90 [28]. The mixed designs of cement and sand ratio of the mortars for bedding and plastering were 1:4 and 1:2, respectively. The compressive strength of the corresponding masonry prism according to ASTM C1314-07 [29] was 7.2 Mpa and 22.0 Mpa, respectively. The brick wall was plastered on both sides with mortar 5 mm. thickness.

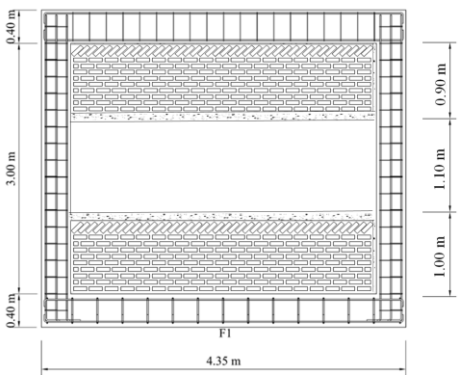

Fig. 7. Infilled frame with central opening.

4.4. Retrofitting of Infilled Frame with Central Opening (FO-R)

The retrofitted frame with opening wall (FO-R) was designed such that the lateral strength is 1.5 times that of the controlled frame (FO). In the design process, the theoretical model of the retrofitted frame with opening presented in the preceding section was also employed in the calculation. The beam-column frame was strengthened with the same process as the bare frame. For the brick wall, each panel was strengthened by the expanded metal type-2 at both sides of the wall. The expanded metal sheet was connected to the wall by small bolts (6.0 mm. diameter) at the spacing of 0.30 m, as shown in Figs. 8a -8d. The finished surface was plastered by cement mortar 1.5 cm. thickness.

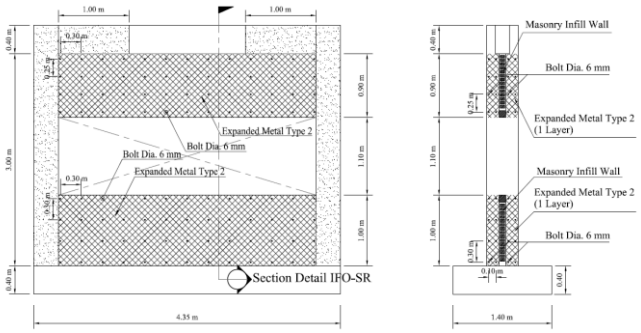

a) Installation of expanded metal b) Cross section

c) Installation of expanded metal d) Plastering of wall

Fig. 8. Retrofitting of infilled frame.

4.5. Experimental Test

The frame sample was supported by the concrete floor connecting with high strength bolts at the footing. The frame was subjected to lateral load by the hydraulic actuator transmitted the load to the concrete wall. The 300 kN vertical axial load was placed on the columns by using hydraulic jacks. The lateral load was applied at the center of beam-column joint. In the positive loading direction, the frame was pushed by the 1500 kN actuator. In the negative loading, the frame was pulled via the 32 mm steel rods. To avoid the transmission of tensile force to the RC beam, high strength steel rods were employed to transfer the drawback force to the frame during the backward direction. The rods were tightened to a steel plate and a steel connector, which was placed at both ends of the frame. The displacement transducers were installed to record the horizontal and vertical displacements of the frame. The transducer (CR) was attached at the top of the frame to record the lateral displacement. At the column

base, the transducers CL1 and CL2 were attached to record the rotation of each side of columns (CR1, CR2). To measure the shear deformation at the column base, the transducers (CL3, CL4) were installed at both sides of columns. To detect the slip between the frame and the base and the rotation of footing, the displacement transducers were placed at the lower end of the frame (FS, FR-R, FR-L). The Test setup for the frame FO-R is presented in Fig. 9. The loading protocol was conducted by displacement control (FEMA 461) [30] with 0.1% drift increment until 0.5% drift. Then the 0.25% drift increment was applied until failure of specimen.

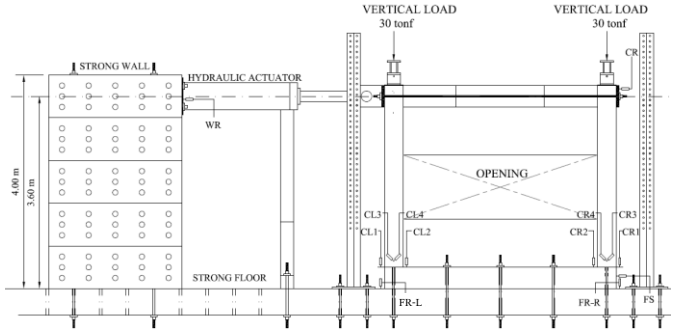

a) Setup for the specimen FO-R

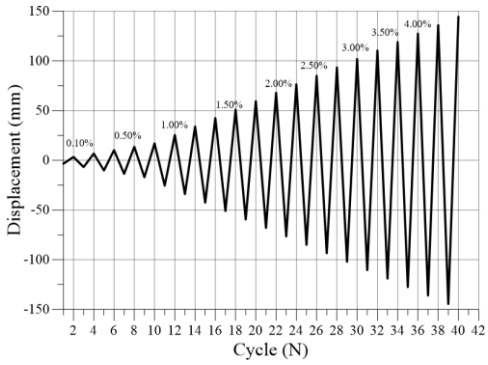

(b) Loading protocol

Fig. 9. Test setup for the specimen FO-R.

5. Experimental Results

5.1. Behavior of Bare Frame (F)

During the early load test, 0.5-1.0% drift, the crack was uncovered at the bottom of the beam-column joint, resulting from the excessive flexural stress. During 1.0-1.5% drift, extensive crack propagate further at the beam ends due to the excessive shear and flexural stress. At the final 2.0% drift, severe crack could be detected at each side of the beam-column joint, displayed in Fig. 10a. Severe damage at the top of both sides of beam ends are presented in Figs. 10b-10c. It is noted that the lateral load resistance of the bare frame is governed by the moment capacity of beam. This is due to the low bending moment capacity of beam (25 kN-m) compared to that of column (102 kN-m).

a) At drift 2.0%

b) Crack at the left beam

c) Crack at the right beam

Fig. 10. Failure of the bare frame (F).

5.2. Behavior of the Retrofitted Frame F-R

During the 0.1-1.0% drift, the frame could sustain the lateral load without any crack. During the 1.0-2.0% drift, the first crack was observed at the right side of the upper beam-column connection as well as the left side. During 2.0-3.0% drift, flexural cracks still occurred at each end of the beam-column connection; however, they did not propagate any further. At the final 4.5 % drift (Fig. 11a), no any additional crack was observed, and only slightly damage could be detected at the beam-column joint (Figs. 11b-11c). It can be noticed that the cracks of the specimen F-R were apparently smaller than those of the bare frame F. The overall specimen still maintained in a good condition which indicated that the ferrocement technique improve the shear-flexure strength of the beam-column connection.

a) At drift 4.5%

DOI:10.4186/ej.2025.29.2.45

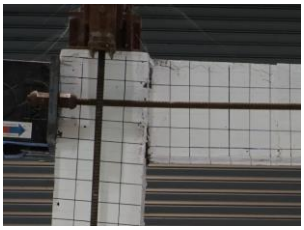
b) Left end


c) Right end

Fig. 11. Failure mechanisms of F-R.

5.3. Behavior of the Opening Frame FO

The first crack was observed at the interface between both upper and lower wall and the adjacent columns, at 0.5% drift, due to the separation of wall and column. Then, at 1.0% drift, the strut force exerted to the column at the lower wall caused the flexural and shear cracks around both columns at the 1.0 meter level above the floor. The crack also propagated to the lower wall. At 2.0% drift, the diagonal crack was noticed at the upper wall due to the diagonal strut force exerted at the right corner of the beam-column, resulting in flexural cracks observed at both ends of the upper columns Finally, the test was terminated at 3.0% drift. Details of failure mechanism are displayed in Figs. 12a – 12e.


a) At drift 3.0%



b) Left upper panel c) Right upper panel



d) Left lower panel e) Right lower panel

Fig. 12. Failure mechanisms of FO.

5.4. Behavior of Retrofitted Opening Frame FO-R

The upper wall panel experienced the first crack at drift level 0.5%, a diagonal crack with an inclination angle about 45 degrees occurred at the right-hand side of wall panel. This crack was due to the diagonal tensile force across the right-hand side portion of the wall. The crack width further propagated with the increase of the drift levels. At the drift level 1.5%, the crack of ferrocement which laminated at the interface between wall panel and column could be observed at both ends of the upper and the lower wall panels. Finally, at the drift level 2.5%, these cracks still maintained at the wall panels until the test was terminated because there was no significant drop of the lateral strength. Details of failure mechanisms are shown in Figs. 13a – 13e. It was observed that no additional crack could be detected in the upper beam and the lower wall. It is noted that the presence of the lower wall panel constrained the lower portion of the columns, and a small flexural crack of column was observed at the height about 1.0 m from the base (Fig. 13d). This indicated that the effect of expanded metal ferrocement prevented the brittle shear failure of column due to the short column effect, and the column exhibited a ductile behaviour with the developed flexural crack at the constrained level.


a) At drift 2.5%


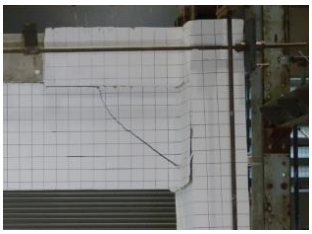
b) Left upper panel c) Right upper panel



d) Left lower column e) Lower wall panel

Fig. 13. Failure mechanisms of FO-R.

5.5. Hysteretic Behaviours of F, F-R, FO and FO-R

The force-displacement relations of the samples F, F-R, FO and FO-R are presented in Figs. 14a, 14b, 14c, 14d, respectively. The behaviour of bare frame F was linearly elastic to 1% drift corresponding to the yield point which is the intersection point of bilinear representation of the enveloped curve. The yield point was determined by the intersection point of the bilinear representation where the area of the segments above and below the curve are approximately equal, suggested by ASCE41-06 [31]. The frame could sustain the lateral load to the maximum strength of 72.46 kN at 1.75% drift. At this stage, the frame was unstable to sustain further loading due to the out-of-plane deviation of the frame. The frame was unsafe for the further test.

For the strengthened bare frame F-R, the system was linear elastic up to the lateral strength of 75 kN, which achieved the yield strength at 1.25% drift. The retrofitted frame sustained the lateral load up to 118 kN at 4.19% drift, where it reached the ultimate strength.

For the controlled frame FO and the retrofitted central opening infilled frame FO-R, the systems showed significant enhancement of both initial stiffness and lateral strength due to the presence of brick wall panel. They were linear elastic up to 0.5% drift, corresponding to the yield strength of 83.59 kN and 171.5 kN, respectively. Then, the stiffness of the frames tended to degrade after this 0.5% drift. Both frames maintained the lateral loads until the drift was about 2.5%, the ultimate lateral strengths reached 105.45 kN and 211.52 kN, respectively.

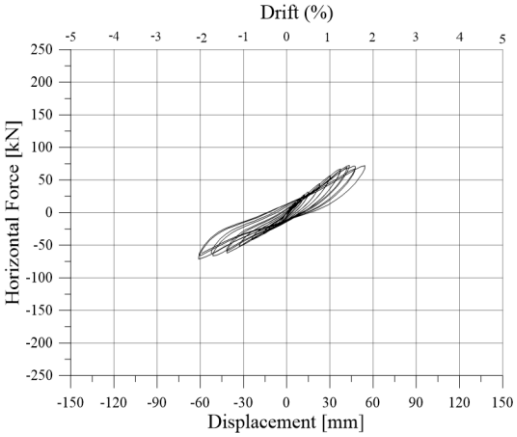

a) Behaviour of bare frame F

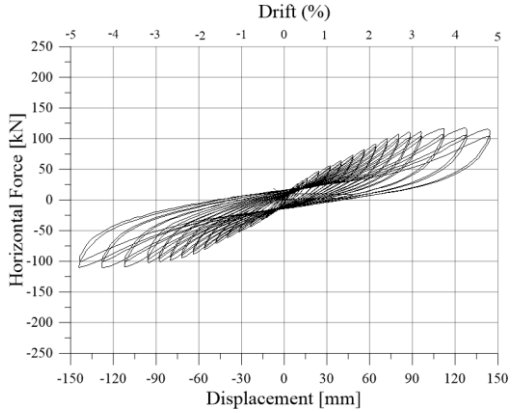

b) Behaviour of retrofitted frame F-R

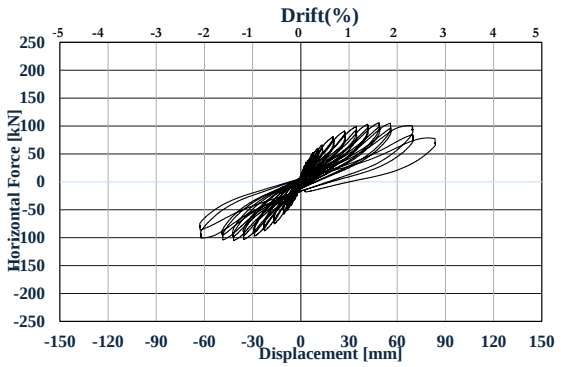

c) Behaviour of central opening frame FO

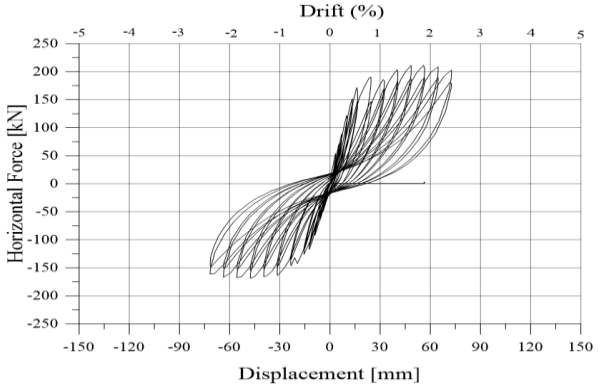

d) Behaviour of retrofitted central opening frame FO-R

Fig. 14. Hysteretic behaviors of tested specimens.

5.6. Lateral Strengths of F, F-R, FO and FO-R

The yield strength and displacement of the frames F, F-R, FO and FO-R are shown in Table 2. Similarly, the ultimate strength, displacement and ductility are shown in Table 3. To determine the efficiency of the retrofitted frame, the retrofit strength (RS) factor was calculated by the ratio of the lateral strength of the retrofitted specimen and that of the controlled sample. For the yield strength level, it appeared that the RS factors of the strengthened bare frame F-R and infilled frame FO-R were 1.50 and 2.05, respectively. Similarly, the RS factors for the ultimate strength of the strengthened bare frame F-R and infilled frame FO-R were 1.69 and 2.00, respectively. It appears that the strength of the retrofitted frames is significantly improved. In addition, the ductility of the strengthened bare frame F-R and infilled frame FO-R were 2.12 and 1.61 times those of the controlled frames, respectively. These indicated that the effects of expanded metal and ferrocement significantly enhanced both of the strength and ductility of the existing frames.

Table 2. Yield strength and displacement for the specimens F, F-R, FO and FO-R.

Specimens	Drift %	Yield strength (kN)	Yield displacement (mm)
F	1.00	50.0	30.0
F-R	1.25	75.0	37.5
FO	0.50	83.59	18.0
FO-R	0.50	171.5	15.0

Table 3. Ultimate strength, displacement and ductility of F, F-R, FO and FO-R.

Sample	Ultimate Strength (kN)	Max. displacement (mm)	Ductility
F	72.46	54.00	1.80
F-R	118.0	143.00	3.81
FO	105.45	48.00	2.67
FO-R	211.52	64.65	4.31

5.7. Lateral Stiffness

The initial stiffness (k_o) which was calculated at the yield strength of the frames F, F-R, FO and FO-R are presented in Table 4. Similarly, the secant stiffness (k_{sec}) was also calculated at the ultimate strength. Among the controlled specimens: F and FO, the presence of masonry infill panel for FO significantly increased the initial and secant stiffness (k_o, k_{sec}) up to 2.00 and 1.64 times those of bare frame F. For the effect of strengthening, the retrofitted infilled frame FO-R enhanced the initial and secant stiffness (k_o, k_{sec}) up to 3.22 and 1.49 times those of the existing frame FO.

Table 4. Initial and secant stiffness (k_o, k_{sec}) for the frames F, F-R, FO and FO-SR.

Sample	Drift level (%)	Initial stiffness (k_o, kN/mm)	Drift level (%)	Secant stiffness (k_{sec} , kN/mm)
F	1.00	1.60	1.75	1.34
F-R	1.25	1.50	4.19	0.83
FO	0.70	3.20	1.70	2.20
FO-R	0.50	10.30	1.90	3.27

The initial stiffness of the frames F, F-R, FO and FO-R are presented in Fig. 15. The stiffness of the frames F, F-R, FO and FO-R decrease with the drift levels because the frames experienced cumulative damage as they sustained the lateral cyclic load. However, the retrofitted specimen FO-R, which is the infill frame with opening, provided the stiffness relatively higher than that of the other specimens due to the effects of the strengthened infill panels including the strengthened beam-column.

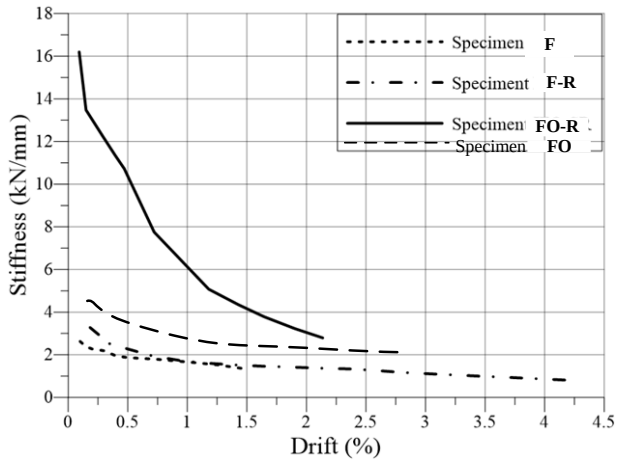

Fig. 15. Stiffness degradation for the specimen F, F-R, FO and FO-R.

5.8. Energy Dissipation

The hysteretic energy of the specimens F, F-R, FO and FO-SR (Fig. 16) provided the normalized energy dissipation which is the cumulative energy dissipation divided by the maximum energy dissipation of the controlled specimen F. The energy dissipation of the strengthened specimens F-R and FO-R are 1.6 and 1.8 times greater than the controlled frame F. The effects of ferrocement reinforced with expanded metal enhance the displacement ductility of the strengthened specimens resulting in the increase of energy dissipation.

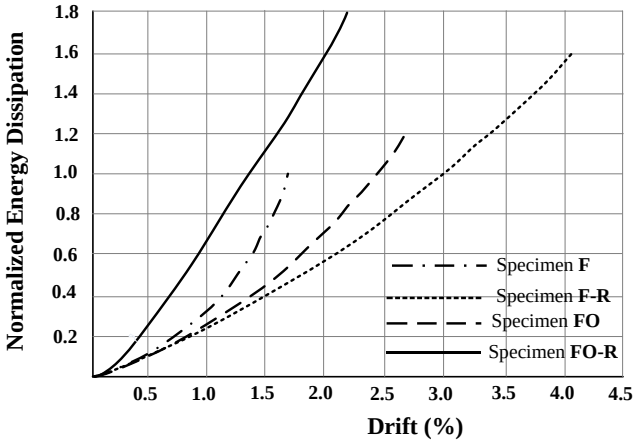

Fig. 16. Energy dissipation for the specimen F, F-R, FO and FO-R.

5.9. Verification of the Proposed Models

To investigate the validity of the proposed models of the strengthened bare frame and the infilled frame with opening. The design strength of the bare frame F, the retrofitted bare frame F-R, and the central opening infilled frame FO, FO-R were calculated. The design strength of the retrofitted bare frame F-R and the infilled frame FO-R are the lateral resistance obtained from Eq. (5) and Eq.

(6) proposed in the model section 3, respectively. For the un-retrofitted bare frame F and the infilled frame FO, Eq. (5) and Eq. (6) can be adapted by employing the properties of the un-retrofitted frame in the corresponding parameters. The calculated design strength of the specimens F and F-R are summarized in Table 5. Details of the internal forces including frame resistance and the strut forces of the upper and the lower wall panels are as follows:

upper wall height $h_1 = 0.90\ m$,

lower wall height $h_2 = 1.00\ m$,

frame height $h = 3.20\ m$, wall length $l_m = 3.65\ m$,

wall thickness $t = 95\ mm$, $\theta_1 = 13.85^o$, $\theta_2 = 15.32^o$,

$\mu = 0.45$, $r = 0.85$, compressive strength of the strengthened masonry prism $f'_m = 8.54 Mpa$,

allowable stress of diagonal strut, $f_a = 3.33\ MPa$,

stress at the corner of infill panel, $\sigma_c = 7.44 Mpa$

plastic moment of connection, $M_{pj} = 24.93\ kN-m$, and plastic moment of column, $M_{pc} = 211.05\ kN-m$.

$\alpha_c = 0.13$

upper strut width w_1 = 113.6 mm

lower strut width w_2 = 125.4 mm

diagonal strut force for the upper panel F_1= 35.94 kN

diagonal strut force for the lower panel F_2 = 39.67 kN

thus, design lateral strength of infill frame

P = 138.81 +35.94 $\cos 13.85^o$ +39.67 $\cos 15.32^o$ =138.81 + 34.90 + 38.26= 211.97 kN.

These are summarized in Table 6. The calculated strut forces for the upper and the lower masonry panels indicated that the total strength of infilled frame increased due to the contribution of the upper and the lower masonry panels. The lateral force transfers the load to the upper panel is greater than the lower one due to the effect of the high stress concentration on the upper masonry panel.

The enveloped curves of hysteretic behaviours for all samples are displayed in Fig. 17. It can be observed that the maximum lateral strength of the bare frame F from the experiment of 72.46 kN is close to the design strength of 74.29 kN. It is expected that the required lateral strength of the strengthened bare frame F-R is 1.5 times that of F, i.e., 111.44 kN. The design lateral strength of the specimen F-R is 138.81 kN. This is slightly greater than the required capacity. The observed maximum lateral strength of the specimen F-R of 118.00 kN reached the required lateral strength of 111.44 kN. However, the obtained strength (118.00 kN) is 15% less than the design lateral strength (138.81 kN) due to the strength degradation of the existing column. The bare frame F has been tested until it reached the ultimate strength, after that the same frame was strengthened to be applied for the specimen F-R. For the infilled frame with opening FO-R, the observed maximum lateral strength of the specimen is 211.52 kN which achieved the design lateral strength of 211.97 kN. These investigations are demonstrated by the enveloped curves of all specimens, as shown in Figure 20. It was found that the design strength based on the proposed model for the retrofitted frame FO-R predicted accurate strength compared to the experimental results.

Table 5. Moment capacity and design strength for the specimens F and F-R.

Parameters	Specimen F	Specimen F-R
Moment capacity of existing column M_E (kN-m)	101.37	101.37
Joint plastic moment M_{pj} (kN-m)	24.93	24.93
Moment capacity of strengthened column M_{sc} (kN-m)	-	211.05
Design strength (kN)	74.29	138.81

Table 6. Design strength of infilled frame from the proposed model.

Parameters	Specimen FO	Specimen FO-R
Frame resistance R_{BF} (kN)	74.29	138.81
Upper Panel $F_1 \cos\theta_1$ (kN)	23.50	34.90
Lower Panel $F_2 \cos\theta_2$ (kN)	20.31	38.26
Design strength P (kN)	118.10	211.97

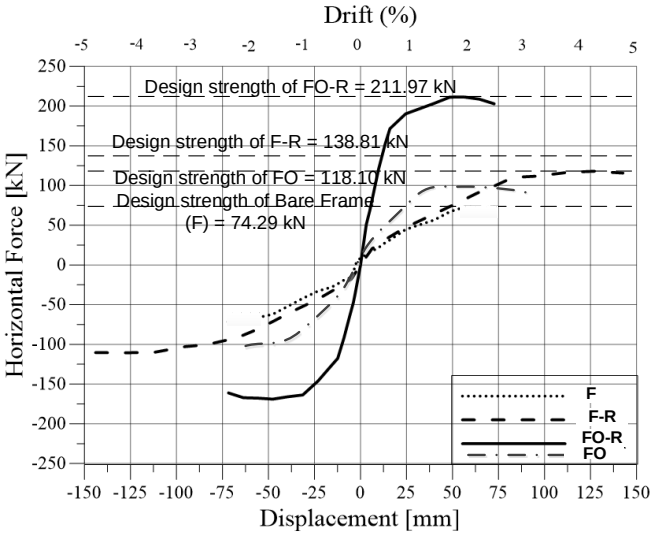

Fig. 17. Enveloped curves for F, F-R, FO and FO-R.

6. Conclusions

The strengthening method for infilled frame with central window opening was presented employing

ferrocement technique. The analytical models were developed for the design of the retrofitted bare frame and the infilled frame with brick wall. The design approach was investigated by the laboratory experiment of the prototype bare frame and the strengthened frames. Based on the presented experimental results, the conclusions are summarized below:

a) Seismic performance of the bare frame and the infilled frame with central opening can be significantly improved. The experimental results reveal that the lateral strength of the retrofitted specimens, which are bare frame and central opening infilled frame, increased up to 1.69 and 2.0 times those of the controlled samples, respectively. The initial and secant stiffness of the strengthened frames enhanced up to 3.22 and 1.49 times, respectively. In addition, the displacement ductility of the retrofitted specimens, bare frame and central opening infilled frame, also increased to 2.12 and 1.61 times those of the controlled samples, respectively.

b) The strengthened columns for the opening infilled frame prevented brittle shear failure due to the behavior of short column. The retrofitted column exhibited a ductile behavior with the developed flexural crack at the constrained level.

c) For the infilled frame with opening FO-R, the observed maximum lateral strength of the specimen (211.52 kN) achieved the design lateral strength (211.97 kN). It was found that the design strength based on the proposed model for the retrofitted frame FO-R predicted accurate strength compared to the experimental results. The proposed analytical models reasonably predicted the lateral strength of the strengthened infilled frame with opening.

d) On the other hand, the observed maximum lateral strength of the strengthened specimen F-R (118.00 kN) reached the required lateral strength of 111.44 kN. However, the obtained strength (118.00 kN) is 15% less than the design lateral strength (138.81 kN) due to the strength degradation of the existing column which has been tested before strengthening.

Acknowledgement

The information of experimental test of this paper is supported by the research project "Behavior, design, and retrofitting of small-sized, medium-sized, and non-engineered buildings for seismically active areas in Thailand", under Thailand Research Fund. The author appreciated kind helpful of all staffs at the laboratory for conducting the experiment.

References

[1] P. Lukkunaprasit, A. Ruangrassamee, T. Boonyatee, C. Chintanapakdee, K. Jankaew, N. Thanasisathit, and T. Chandrangsu, "Performance of structures in the Mw 6.1 Mae Lao earthquake in Thailand on May 5, 2014 and implications for future construction," *Journal of Earthquake Engineering*, vol. 20, no. 2, pp. 219-242, 2016.

[2] Federal Emergency Management Agency, "Evaluation of earthquake damaged concrete and masonry wall building," Federal Emergency Management Agency, FEMA 306, Washington D.C., 1998.

[3] E. Sleiman, E. Ferrier, L. Michel, and M. Saidi, "Seismic behavior of masonry-infilled reinforced concrete frames strengthened using ultra-high performance concrete diagonal strips," *Structures*, vol. 59, p. 105790, 2024.

[4] M. G. Azandariani and A. Mohebkhah, "A multi-strut model for the hysteresis behavior and strength assessment of masonry-infilled steel frames with openings under in-plane lateral loading," *Engineering Structures*, vol. 302, p. 117433, 2024.

[5] C. Ozkan, M. S. Okten, M. Gencoglu, and B. Sayin, "Seismic upgrading of infilled RC frames having low concrete strength using engineered composites under cyclic and axial loading," *Structures*, vol. 58, p. 105586, 2023.

[6] M. H. Ahmadi and F. N. Alahi, "Experimental investigation of strengthening of masonry-infilled RC frames using prefabricated engineered cementitious composite panels," *Engineering Structures*, vol. 253, p. 113762, 2022.

[7] J. K. Bhaskar, D. Bhunia and L. Koutas, "In-plane behavior of masonry infill walls with opening strengthened using textile reinforced mortar," *Structures*, vol. 63, p. 106439, 2024.

[8] H. T. Kabaş, F. E. Kusain, and O. Anıl, "Experimental behavior of masonry infilled RC frames with openings strengthened by using CFRP strip," *Composite Structures*, vol. 312, p. 116873, 2023.

[9] M. Batikha and F. Alkam, "The effect of mechanical properties of masonry on the behavior of FRP-strengthened masonry-infilled RC frame under cyclic load," *Composite Structures*, vol. 134, pp. 513-522, 2015.

[10] G. Erol and H. Karadogan, "Seismic strengthening of infilled reinforced concrete frames by CFRP," *Composites Part B: Engineering*, vol. 91, pp. 473-491, 2016.

[11] C. G. Papanicolaou, T. C. Triantafillou, M. Papathanasiou, and K. Karlos, "Textile reinforced mortar (TRM) versus FRP as strengthening material of URM walls: out-of-plane cyclic loading," *Materials and Structures*, vol. 41, no. 1, pp. 143–57, 2008.

[12] *Standards for Expanded Metal*, EMMA 557-12, Expanded Metal Manufacturers Association (EMMA), 2012.

[13] M. T. Kazemi and R. Morshed, "Seismic shear strengthening of R/C columns with ferrocement jacket," *Cement & Concrete Composites*, vol. 27, pp. 834–42, 2005.

[14] P. N. Dung and A. Plumier, "Behaviour of expanded metal panels under shear loading," in *Proceedings of*

SDSS RIO 2010 Stability and Ductility of Steel Structures, Rio de Janeiro, 2010, pp. 1101–1108.
[15] P. Teixeira, G. Martinez, and C. Graciano, "Shear response of expanded metal panels," *Engineering Structures,* vol. 106, pp. 261-272, 2016.
[16] A. Leeanansaksiri, P. Panyakapo, and A. Ruangrassamee, "Seismic capacity of masonry infilled RC frame strengthening with expanded metal ferrocement," *Engineering Structures*, vol. 159, pp. 110–127, 2018.
[17] S. Longthong, P. Panyakapo, and A. Ruangrassamee, "Seismic strengthening of RC frame and brick infill panel using ferrocement and expanded metal," *Engineering Journal*, vol. 24, no. 3, pp. 45-59, 2020.
[18] B. Aykac, E. Ozbek, R. Babayani, M. Baran, and S. Aykac, "Seismic strengthening of infill walls with perforated steel plates," *Engineering Structures*, vol. 152, pp. 168–179, 2017.
[19] S. Panyamul, P. Panyakapo, and A. Ruangrassamee, "Seismic shear strengthening of reinforced concrete short columns using ferrocement with expanded metal," *Engineering Journal*, vol. 23, no. 6, pp. 175-189, 2019.
[20] P. Nagaprasad, D. R. Sahoo, and D. C. Rai, "Seismic strengthening of RC column using external steel cage," *Earthquake Engineering and Structural Dynamics*, vol. 38, pp. 1563-1586, 2009.
[21] R. Amornpunyapat, P. Panyakapo, and M. Panyakapo, "Development of lightweight concrete interlocking block panel with water treatment sludge and expanded metal ferrocement," *Engineering Journal*, vol. 25, no. 1, pp. 81-97, 2021.
[22] P. Panyakapo, "Seismic analysis of RC frames with brick infill panel strengthened by steel cage and expanded metal," *Engineering Journal*, vol. 25, no. 4, pp. 29-44, 2021.
[23] *Standard for Reinforced Concrete Building (Working Stress Design Method)*, EIT Standard 1007-34, Engineering Institute of Thailand, Bangkok, Thailand, 1991.
[24] *Building Code Requirements for Reinforced*, ACI Standard No. ACI318, American Concrete Institute (ACI), 1995.
[25] *Guide for the Design, Construction, and Repair of Ferrocement*, ACI 549.1R-93, American Concrete Institute (ACI), 1999.
[26] A. Saneinejad and B. Hobbs, "Inelastic design of infilled frames," *Journal of Structural Engineering*, vol. 6682, pp. 634-50, 1995.
[27] *Expanded Metal Standard by Japanese Industrial Standard*, JIS Standard No. JIS G3351, Japanese Standards Association (JIS).1987.
[28] *Standard Test Method for Compressive Strength of Dimension Stone*, ASTM C170, American Society for Testing and Materials (ASTM), 2001.
[29] *Standard Test Method for Compressive Strength of Masonry Prisms*, ASTM C1314, American Society for Testing and Materials (ASTM). 2007.
[30] Interim Testing Protocol for Determining the Seismic Performance Characteristics of Structural and Nonstructural Components, FEMA 461, Federal Emergency Management Agency, Redwood City, 2007.
[31] *Seismic Rehabilitation of Existing Building*, ASCE Standard No. ASCE/SEI 41–06, American Society of Civil Engineers (ASCE), 2007.

Phaiboon Panyakapo hold Doctor of Engineering from AIT since 1999. He has been graciously recieved Professor of Civil Eng. since 2018. He is a committe in the Engineering Institute of Thailand. He also involved in the improvement of earthquake resistant design standard of Thailand. His research involed in the seismic analysis and design, seismic strengthening of building.